MADRID
inter.noise 2019
June 16 - 19
NOISE CONTROL FOR A BETTER ENVIRONMENT

Analytical Study on Dynamics of Wedge Braking Systems with Time Delay

Qiang Liu, Li Chen*, Jun Chen

State Key Laboratory of Ocean Engineering, Collaborative Innovation Center for Advanced Ship and Deep-Sea Exploration, Shanghai Jiao Tong University, Shanghai 200240, P.R. China

ABSTRACT

Wedge brakes enlighten new concepts of automotive braking systems because large friction braking force can be generated by small actuation force. A dynamic model with time-delayed feedback is built for the wedge braking system. The multiscale method is adopted to obtain the analytical solution of the primary resonance response. The Routh-Hurwitz criterion is used to analysis the stability. The influences of time delay, wedge angle and system stiffness on the dynamic response and stability are examined. The analytical solution is verified by the numerical solution. The analytical results show that the amplitude of the stable state and the stability boundary periodically varies along with the time delay. Within one period, large time delay induces saddle-node bifurcation and leads to instability. Moreover, larger wedge angle and larger stiffness significantly increase the amplitude of the stable state, and expand the instable region. The method and results provide reference for design and control of wedge-based braking systems.

Keywords: Time delay dynamics, Wedge brake, Stability
INCE Classification of Subject Number: 41

1. INTRODUCTION

Compared with the conventional brake, the wedge brake utilizes the self-energizing characteristic[1] of the wedge to produce enough braking torque with a small actuation force. Thus, the size and losses of the actuation motor can be reduced[2-4]. Research on traditional brakes shows that the friction braking system may have chattering and squeal noise, which seriously affects the braking process and service life[5, 6]. During the braking process, the friction state of friction interface transitions from sliding to sticking. Since the produced friction is asymmetric due to the self-energizing ratio is related to the direction of relative velocity, the dynamic response at the stick-slip events exhibits a asymmetry characteristic[7]. Moreover, the inevitable time delay in braking torque control and application, such as signal transmission delay and actuator delay, also has a complex impact on the dynamics of the braking system, thus, the mechanism needs to be further studied.

Until now the research on dynamics of the wedge braking system has never considered the time-delay effect[8-11]. Studies on general nonlinear dynamic systems

[1] lqstudyinsjtu@sjtu.cn
[2] li.h.chen@sjtu.edu.cn
[3] jun_ch1225@sjtu.edu.cn

have shown that time delay may cause bifurcation, and lead to instability[12, 13]. Applying the nonlinear method to solve the problem is convenient for analyzing the dynamic response. Yaman[14] et al. studied the effect of feedback gain and time delay on the steady state resonance response of nonlinear cantilever beam by using multiscale method. Chatterjee[15] et al. built and solved the time-delay dynamic model of friction-induced vibration by using KBM asymptotic method, and carried out the stability analysis. Zhao[16] et al. applied perturbation method to analyze amplitude-frequency response and stability of time-delay dynamic vibration absorber. Sun[17] et al. analyzed the influence of system control gain and time delay on the saturation control damping band, and proposed a method to improve the performance of the dynamic vibration absorber based on these results. Saha[18] et al. applied the multiscale method to solve the time-delay dynamic model of the belt-spring-mass system with LuGre friction model, and obtained the bifurcation characteristics of the system. Referring to these papers, we use the multiscale method to solve the dynamic response of the wedge-type braking system near the stick-slip events under time delay effect, and further analyze its stability and dynamic behaviour.

For the friction-induced dynamic problem, the traditional Coulomb friction model is discontinuous and non-differentiable at zero relative velocity, which brings difficulties to modelling and solving process. According to the type of friction model, the literature on the dynamic analysis of the wedge braking system can be divided into two categories, one of which only considers the cases that the direction of relative velocity on the friction interface keep positive or negative, avoiding the problem of discontinuity. Hwang[19], Roberts[20] and Mahmoud[21] respectively studied the impact of brake pressure, the motor voltage, wedge angle, etc. on the dynamic response under unidirection friction. The other type of studies utilizes the smooth function to fit the discontinuous friction model. Balogh[22] et al. designed a S-type function(Sigmoid) to fit the Coulomb friction model and calculated the pressure, displacement and friction generated by the wedge control system under different control inputs. Li et al. designed hyperbolic tangent smooth function, and used this model calculate the dynamic response under different wedge angle and feedback control gain. This smoothing model is also applied to other friction-induced dynamics problem[23, 24]. However, the existing smooth functions usually contain complex function such as exponential and hyperbolic tangent, which can be applied to numerical calculation but require further simplification to be applicable to analytical calculation.

This paper established the nonlinear time-delay model of wedge braking system, the friction model was established by using a combination of smoothing function and polynomial fitting method. Then the multiscale method is applied to obtain the analytical solution, and the Routh-Hurwitz criterion is adopted to analyze the stability boundary. The impact of time delay, system stiffness and wedge angle on the amplitude-frequency curve is discussed based on the analytical solution.

2. DYNAMICS MODEL WITH TIME DELAY

2.1 Wedge brake governing equation

The working principle of wedge brake is shown in Fig.1[7], the motor pushes the wedge in contact with the brake disc, generating friction force on the friction interface, thus, the brake disc gradually stop rotating.

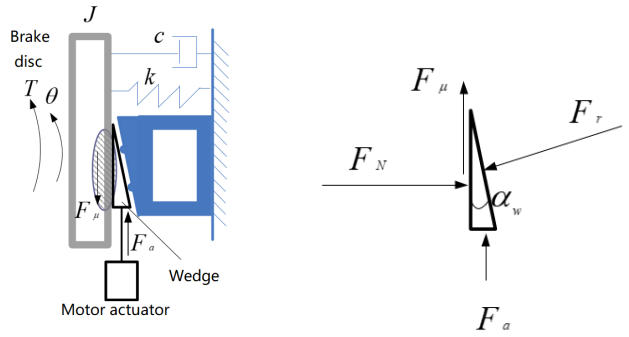

（a）Brake actuation principle　　（b）equilibrium condition of forces

Fig.1 Working principle of wedge brake

The dynamic equation of brake disc affected by the wedge can be expressed as

$$J\ddot{\theta}(t)+c\dot{\theta}(t)+k\theta(t)+RF_{\mu}(t-\tau)=T(t) \tag{1}$$

Where F_N、F_r are the normal pressure on the wedge，F_a is the action force of the driveline，F_{μ} is the friction force on the friction interface，α_w is the wedge angle，J、c、k are the moment of inertia、damping and stiffness of the driveline respectively，R is the equivalent radius of the friction force，T is the external torque with amplitude is T_e and frequency is f_e.

$$T(t)=T_e\cos(\Omega t) \tag{2}$$

$$\Omega=2\pi f_e \tag{3}$$

2.2 Friction model

Applying the Coulomb friction model, the friction coefficient can be expressed as

$$\mu(v)=\begin{cases}\mu_k\,\mathrm{sign}(v) & v\neq 0\\ [-\mu_s\ \ \mu_s] & v=0\end{cases} \tag{4}$$

Where μ_k is kinetic friction coefficient and μ_s is static friction coefficient. The relative sliding speed on the friction interface is calculated by the angular velocity of the brake disc.

$$v=R\dot{\theta} \tag{5}$$

The positive pressure of wedge satisfies the following equations.

$$(F_{\mu}+F_a)/F_N=\tan(\alpha_w) \tag{6}$$

$$F_a=F_{a0}+\delta\,\mathrm{abs}(v) \tag{7}$$

$$F_{\mu}=\mu(v)F_N \tag{8}$$

Where δ is the slope of F_a, and F_{a0} is the initial value of F_a. From (4), (6), (7), (8), the friction on the friction interface can be derived as

$$F_\mu = \begin{cases} F_a\mu_k \operatorname{sign}(v) / \left(\tan(\alpha_w) - \mu_k \operatorname{sign}(v)\right) & v \neq 0 \\ \left[-F_a\mu_s / \left(\tan(\alpha_w) - \mu_s\right) \quad F_a\mu_s / \left(\tan(\alpha_w) - \mu_s\right)\right] & v = 0 \end{cases} \tag{9}$$

Where the case of $\tan(\alpha_w) < \mu_s$ is not discussed in this paper because it will lead to instability in the wedge mechanism design.

However, the friction of (9) is discontinuous, thus, a smoothened model[25] is adopted to deal with it.

$$\mu'(v) = \left(1 + \left(\frac{\mu_s}{\mu_k} - 1\right) e^{-\zeta \operatorname{abs}(v)}\right) \tanh(\xi v)\, \mu_k \tag{10}$$

Where ζ and ξ are tuning parameters, given $\zeta = 15$ and $\xi = 30$. The result of fitting the smoothened model to the Coulomb friction model is shown in Fig.2(a).

It is noted that the smoothened model of equation (10) contains an exponential function and a hyperbolic function, which is inconvenient for the derivation of the nonlinear analytical method. This paper focuses on the dynamic response near the stick-slip events (ie, the relative velocity of the friction interface is small), in which the friction model can be fitted with a cubic polynomial, the expression is as follows and the fitting results are shown in Fig.2(b).

$$\mu''(v) = \alpha v + \beta v^2 + \gamma v^3 + \lambda \tag{11}$$

Thus, the friction in (9) can be expressed as:

$$F_\mu(v) = F_a \mu(v) \Big/ \left(\tan(\alpha_w) - \mu(v)\right) \tag{12}$$

The ratio of friction F_μ to driving force F_a reflects the "self-energizing" effect and the asymmetry characteristic of the wedge, which is shown in Fig.2(c), given $\alpha_w = 0.34$, $\mu_k = 0.3$, $\mu_s = 0.33$, $F_a = 250N$.

The time delay of motor and actuator is introduced as a variable to describe the delay effect, thus, $\theta_\tau = \theta(t-\tau)$, $F_\mu = F_\mu(t-\tau)$, $F_a = F_a(t-\tau)$. Substituting $\mu = c/J$, $\omega^2 = k/J$, we obtain the normalized model

$$\ddot{\theta} + \mu\dot{\theta} + \omega^2\theta + R\left(\alpha\dot{\theta}_\tau + \beta\dot{\theta}_\tau^2 + \gamma\dot{\theta}_\tau^3 + \lambda\right) \Big/ J = T(t)/J \tag{13}$$

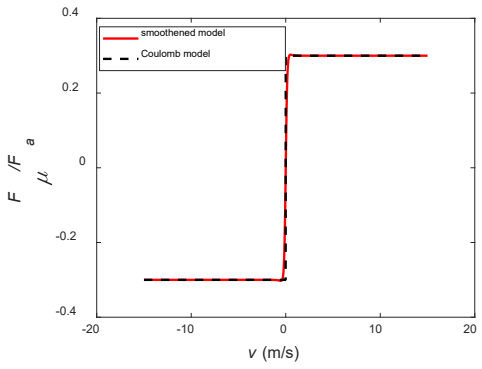

（a）Coulomb model and smoothened model

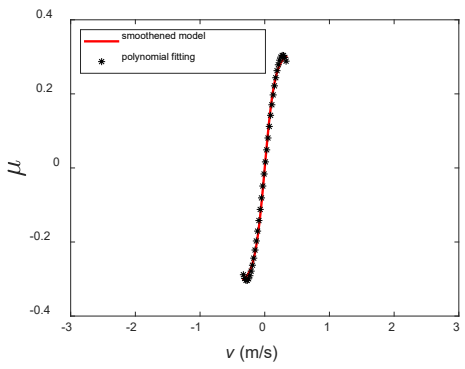

（b）Smoothened model and its polynomial fitting

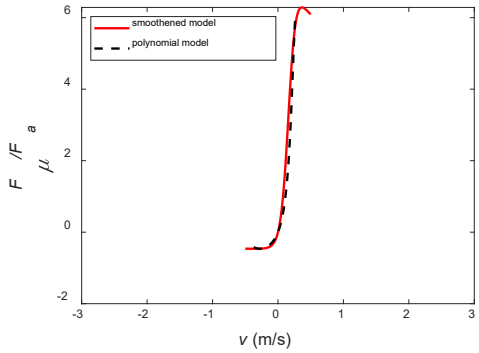

（c）Characteristics of friction force on the wedge

Fig.2 modeling of the friction force on the wedge

3. FORCED PRIMARY RESONANCE ANALYSIS

3.1 Multiscale method

For convenience, substituting

$$\theta = x + \frac{R\lambda}{J\omega^2} \tag{14}$$

Thus, $\theta_\tau = x_\tau + R\lambda / J\omega^2$. Substituting (14) into (13) and introducing a small parameter ε ($0<\varepsilon<1$), the equation (13) can be transformed as a small perturbation model.

$$\ddot{x} + \omega^2 x = \varepsilon\left(T_e \cos(\Omega t) + \alpha\dot{x}_\tau + \beta\dot{x}_\tau^2 + \gamma\dot{x}_\tau^3 - \mu\dot{x}\right) \tag{15}$$

Introducing two different time scales, $T_0 = t, T_1 = \varepsilon t$, and a partial derivative operator

$$\frac{\mathrm{d}}{\mathrm{d}t} = D_0 + \varepsilon D_1 + \ldots \tag{16}$$

$$\frac{\mathrm{d}^2}{\mathrm{d}t^2} = D_0^2 + 2\varepsilon D_0 D_1 + \ldots$$

Substituting Eq. (16) in (15), and separating the terms which have the same exponential of ε , the following equation can be derived.

$$D_0^2 x_0 + \omega_0^2 x_0 = 0 \tag{17}$$

$$D_0^2 x_1 + \omega^2 x_1 = -2D_0 D_1 x_0 - \mu D_0 x_0 + \alpha\dot{x}_\tau + \beta\dot{x}_\tau^2 + \gamma\dot{x}_\tau^3 + T_e \cos(\Omega t) \tag{18}$$

The approximate solution of Eq.(17) can be expressed as follows

$$x_0(T_0, T_1) = A_\tau(T_1) e^{i\omega T_0} + cc \tag{19}$$

Where cc is the complex conjugate of the previous term. The external excitation term and the time delay term can be expressed as follows

$$T_e \cos(\Omega t) = \frac{1}{2} T_e e^{i\Omega T_0} + cc \tag{20}$$

$$x_\tau = A_\tau(T_1) e^{i\omega(T_0 - \tau)} + cc \tag{21}$$

In order to obtain the first order approximate solution $x_1(T_0,T_1)$, we substituting the Eq.(19)、(20)、(21) in (18) at first.

$$\begin{aligned}\left(D_0^2+\omega^2\right)x_1 &= -2i\omega D_1 A(T_1)e^{i\omega T_0} - \mu i\omega A(T_1)e^{i\omega T_0} + \frac{1}{2}T_e e^{i\Omega T_0} \\ &+\alpha i\omega A e^{i\omega(T_0-\tau)} + \beta\left(-\omega^2 A^2 e^{2i\omega(T_0-\tau)} + \omega^2 A\overline{A}\right) \\ &+\gamma\left(-i\omega^3 A^3 e^{3i\omega(T_0-\tau)} + 3i\omega^3 A^2\overline{A}e^{i\omega(T_0-\tau)}\right) + cc\end{aligned} \tag{22}$$

A tuning parameter σ is introduced to describe the deviation between excitation frequency and natural frequency.

$$\Omega=\omega+\varepsilon\sigma \tag{23}$$

To eliminate the secular term， we set the sum of the coefficient with $e^{i\omega T_0}$ in it's term equal to 0：

$$-2i\omega D_1 A(T_1) - \mu i\omega A(T_1) + \frac{1}{2}T_e e^{i\sigma T_1} + \alpha i\omega A e^{-i\omega\tau} + 3\gamma i\omega^3 A^2\overline{A}e^{-i\omega\tau} = 0 \tag{24}$$

The amplitude can be expressed in polar form as

$$A(T_1) = \frac{1}{2}a(T_1)e^{i\eta(T_1)} \tag{25}$$

Substituting $\varphi=\sigma T_1-\eta$ and Eq. (25) in (24), and separating the imaginary parts and real parts, we can obtain the following equation.

$$a' = -\frac{1}{2}\mu a + \frac{1}{2}\alpha a\cos(\omega\tau) + \frac{3}{8}\gamma a^3\omega^2\cos(\omega\tau) + \frac{1}{2\omega}T_e\sin(\sigma T_1-\eta) \tag{26}$$

$$a\varphi' = a\sigma + \frac{1}{2}\alpha a\sin(\omega\tau) + \frac{3}{8}\gamma a^3\omega^2\sin(\omega\tau) + \frac{1}{2\omega}T_e\cos(\sigma T_1-\eta) \tag{27}$$

3.2 Amplitude-frequency response equation

Substituting the right side of Eq. (26) and (27) with zero, we can obtain the amplitude and phase of steady state solution.

$$\frac{1}{2\omega}T_e\sin(\varphi) = \frac{1}{2}\mu a - \frac{1}{2}\alpha a\cos(\omega\tau) - \frac{3}{8}\gamma a^3\omega^2\cos(\omega\tau) \tag{28}$$

$$\frac{1}{2\omega}T_e\cos(\varphi) = -a\sigma - \frac{1}{2}\alpha a\sin(\omega\tau) - \frac{3}{8}\gamma a^3\omega^2\sin(\omega\tau) \tag{29}$$

To eliminate the variable φ, calculate the quadratic sum of Eq.(28) and (29), and the amplitude-frequency response equation is derived as

$$\begin{aligned}\frac{T_e^2}{4\omega^2} &= \left(\frac{1}{2}\mu a - \frac{1}{2}\alpha a\cos(\omega\tau) - \frac{3}{8}\gamma a^3\omega^2\cos(\omega\tau)\right)^2 \\ &+\left(-a\sigma - \frac{1}{2}\alpha a\sin(\omega\tau) - \frac{3}{8}\gamma a^3\omega^2\sin(\omega\tau)\right)^2\end{aligned} \tag{30}$$

3.3 Stability analysis

Substituting $a^{'}=f_1(a,\varphi),\varphi^{'}=f_2(a,\varphi)$ in Eq.(26) and (27), the Frechet derivative of which is given by

$$F^{'}(x)=\begin{vmatrix}\dfrac{\partial f_1}{\partial a} & \dfrac{\partial f_1}{\partial \varphi}\\ \dfrac{\partial f_2}{\partial a} & \dfrac{\partial f_2}{\partial \varphi}\end{vmatrix} \tag{31}$$

where

$$\frac{\partial f_1}{\partial a}=-\frac{1}{2}\mu+\frac{1}{2}\alpha\cos(\omega\tau)+\frac{9}{8}\gamma a^2\omega^2\cos(\omega\tau) \tag{32}$$

$$\frac{\partial f_1}{\partial \varphi}=-a\sigma-\frac{1}{2}\alpha a\sin(\omega\tau)-\frac{3}{8}\gamma a^3\omega^2\sin(\omega\tau) \tag{33}$$

$$\frac{\partial f_2}{\partial a}=\frac{1}{a}\left(\sigma-\frac{1}{2}\alpha\sin(\omega\tau)+\frac{9}{8}\gamma a^2\omega^2\sin(\omega\tau)\right) \tag{34}$$

$$\frac{\partial f_2}{\partial \varphi}=-\frac{1}{2}\mu+\frac{1}{2}\alpha\cos(\omega\tau)+\frac{3}{8}\gamma a^2\omega^2\cos(\omega\tau) \tag{35}$$

For convenience, we substituting these terms as

$$A=\frac{\partial f_1}{\partial a},B=\frac{\partial f_1}{\partial \varphi},C=\frac{\partial f_2}{\partial a},D=\frac{\partial f_2}{\partial \varphi} \tag{36}$$

The characteristic equation corresponding to the differential equations is given by

$$\lambda^2+(A+D)\lambda+AD-BC=0 \tag{37}$$

Where λ is the eigenvalue of the equation. From the Eq.(37), we can obtain the sum of two roots is $-(A+D)$, which is related to friction coefficient, time delay, natural frequency, wedge angle, etc. According to Routh-Hurwitz criterion, if $A+D>0$ and $AD-BC>0$, the steady state solution is stable, and there is no frequency hopping in the system. If $AD-BC=0$, the system is in stability boundary condition, which will generate saddle-node bifurcation and the amplitude-frequency response curve will appear unstable region

4. RESULTS ANALYSIS

Parameters are selected as follows: c=1Nms/rad, J=1kgm^2, k=10000Nm/rad, T_e =150N, R=0.2m, δ=0. The results of multiscale method are analyzed in this section. The amplitude-frequency response curve and stability vary with different time delay, wedge angle and stiffness of the driveline is discussed. Finally, the analytical solution and numerical solution are compared to validate the calculation.

4.1 Influence of time delay on amplitude-frequency response curve

According to Eq.(30) we can obtain amplitude-frequency response curves vary with different time delay, which is shown in Fig.3.

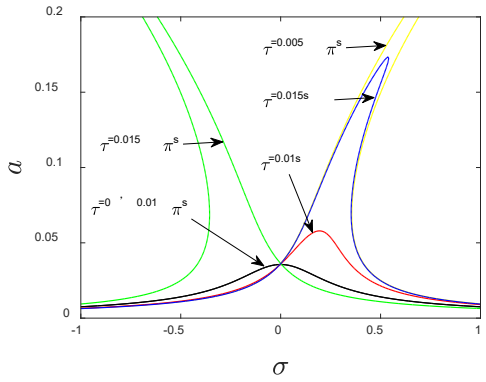

Fig.3 Amplitude-frequency response under different time delay

We observe from Fig.3 that with the increase the time delay τ, when $0<\tau<0.005\pi$s, the primary resonance frequency and amplitude increase continuously, and the multi-stable solution begins to appear. The hard stiffness characteristic of the system is more obvious, which is due to the cubic term in the model. When $0.005\pi s<\tau<0.01\pi$s, the primary resonance frequency and amplitude decrease continuously. When $0.01\pi s<\tau<0.015\pi$s, the primary resonance curve begin to bend to the other side and the soft stiffness characteristic is more obvious. In this case, the cubic term is also the expansion term of the friction force, so there is a time delay in the cubic term, and the value of the time delay will affect the soft and hard characteristics of the system.

To further analyze the influence of time delay on amplitude-frequency response curve, the system amplitude - delay response and stability boundary are given in Fig.4 and Fig.5.

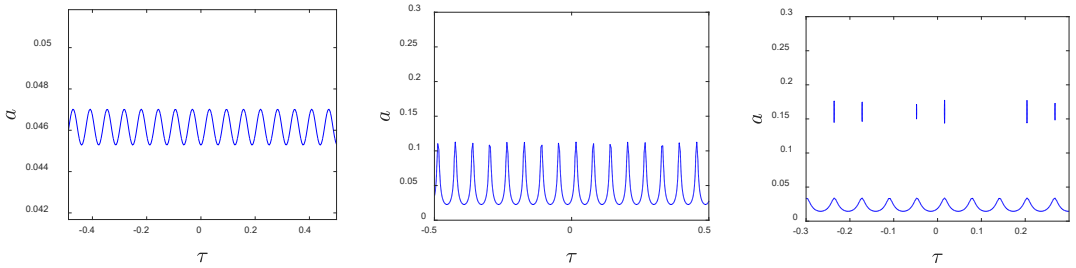

（a）σ = 0　　（b）σ = 0.25　　（c）σ = 0.5

Fig.4 System amplitude - delay response

As can be seen in Fig.4(a) and (b) , when σ=0 and σ=0.25, the primary resonance amplitude shows a periodic variation. The primary resonance amplitude decreases in some time delay interval, indicating that it can be reduced by controlling time delay. When σ=0.5, the primary resonance amplitude has multiple solutions, that is, the amplitude has a hopping phenomenon.

The amplitude-frequency response curve can be obtained according to Eq.(30) and stability boundary, which is shown in Fig.5.

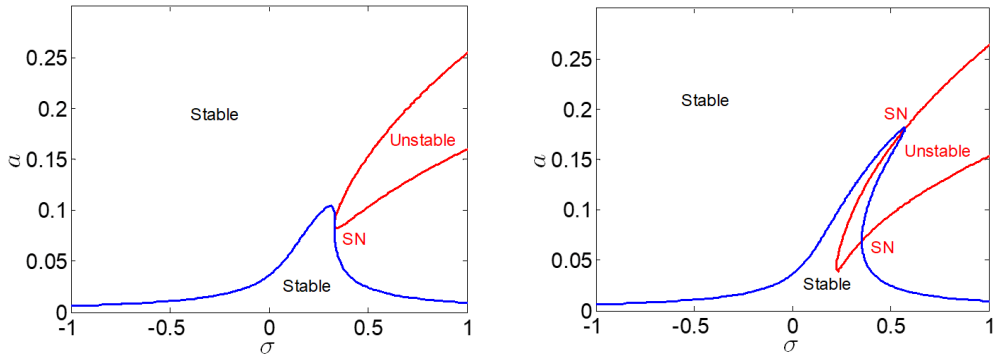

（a）$\tau = 0.0134\text{s}, \alpha = 0.34$　　（b）$\tau = 0.015\text{s}, \alpha = 0.34$

Fig.5 The effect of time delay on stability

The solid red line in Fig.5 is stability boundary, the inner part of which is unstable region while the outer part is stable. The intersection of two curves(SN) is saddle-node bifurcation point, and the braking process in this area is prone to chatter. When τ=0, the system is in a stable region. When 0<τ <0.005πs, with the increase of time delay, the unstable region curve also expands. The amplitude-frequency response curve and stability boundary begin to intersect at τ=0.0134s. There is only one stable solution to the system on the left side of saddle-node bifurcation point while three on the right side, of which the upper solution branch and the lower solution branch are both stable solutions, while the solution in the middle intersecting unstable region is unstable. When 0.005π<τ <0.01πs, with the increase of time delay, the unstable region of the system decreases and the stability factor increases. We can also conclude that the primary resonance amplitude can be reduced and the unstable region can be eliminated by controlling time delay.

4.2 Influence of wedge angle on amplitude-frequency response curve

Wedge angle is a significant parameter in the wedge mechanism design. Improper selection of angle will cause the required restoring force is too large, and even the wedge cannot be returned smoothly, so that the car is always in a braking state. The influence of wedge angle on amplitude-frequency response curve is shown in Fig.6.

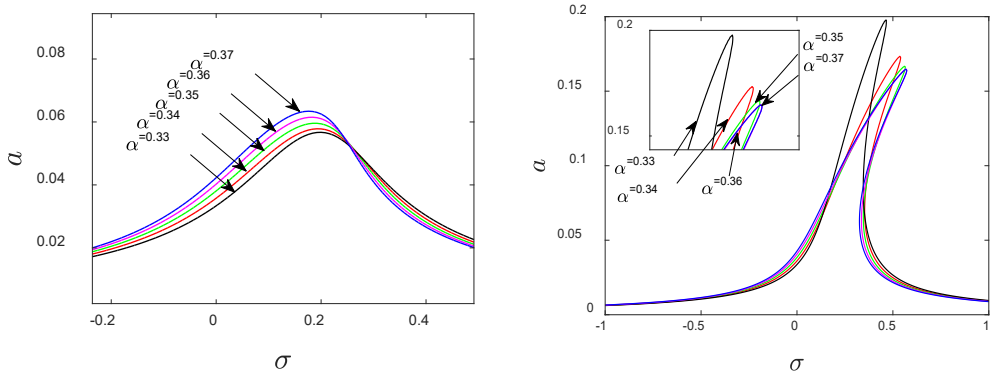

（a）$\tau = 0.01\text{s}$　　（b）$\tau = 0.015\text{s}$

Fig.6 Amplitude-frequency response at different wedge angles

We can observe from Fig.6 that wedge angle and the amplitude-frequency response curve is closely related. When time delay is relatively small, the primary resonance amplitude increase slightly with the increase of wedge angle α_w. With the

increase of time delay, the unstable region become larger, which indicates that the primary resonance amplitude and the system stability can be controlled within the acceptable range by appropriately reducing the wedge Angle.

4.3 Influence of system stiffness on amplitude-frequency response curve

Wedge braking system stiffness can affect the natural frequency, so that the forced vibration will also be impacted. The relationship between system stiffness and amplitude frequency response curve is shown in Fig.7.

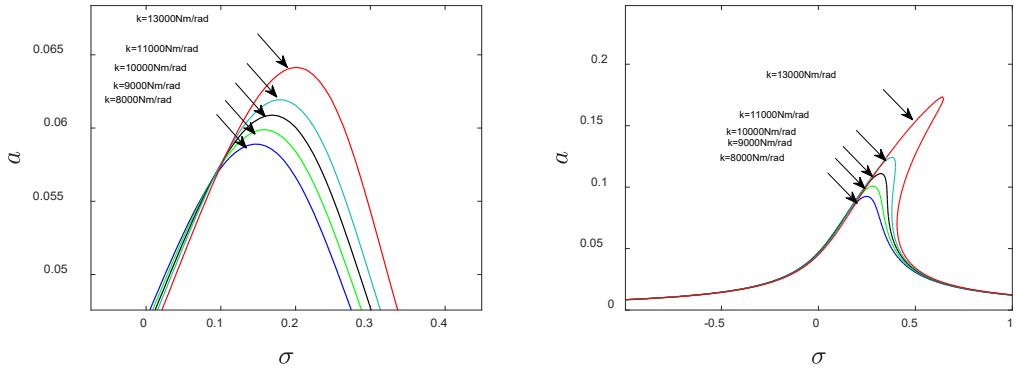

（a）$\tau = 0.01\text{s}, \alpha = 0.34$　　（b）$\tau = 0.014\text{s}, \alpha = 0.34$

Fig.7 The effect of system stiffness on stability

As can be seen in Fig.7, with the increase of the system stiffness, the primary resonance amplitude also increases, and this change is amplified with the increase of time delay. In some cases(e.g. Fig.7(b)), the amplitude-frequency response curve appears unstable solution branch, and the unstable region expands with the increase of system stiffness, which should be avoided when designing wedge brake.

4.4 Comparison between numerical solution and analytical solution

The correctness of analytical solution can be verified by comparing with numerical solution based on Eq.(1). When $\tau = 0.01\text{s}$, and the external excitation frequency is equal to natural frequency, the analytical in time domain can be derived as

$$x = a\cos\left(\omega\left(t-\tau\right)+\varphi\right)+\frac{\varepsilon\beta a^2}{2} + \frac{\varepsilon\beta a^2}{6}\cos\left(2\omega\left(t-\tau\right)+\varphi\right)-\frac{\varepsilon\gamma\omega a^3}{32}\sin\left(2\omega\left(t-\tau\right)+\varphi\right) \tag{38}$$

The comparison between the numerical solution and the analytical solution in steady state is shown in Fig. 9, which shows that they are basically consistent.

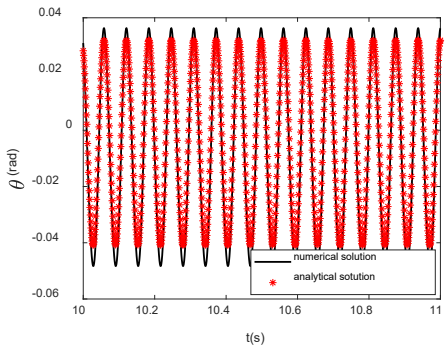

Fig.8 Comparison between numerical solution and analytical solution($\tau = 0.01\text{s},, \sigma = 0$)

When $\sigma \neq 0$, the following two cases are chosen to compared with amplitude-frequency response curve in Fig.9.

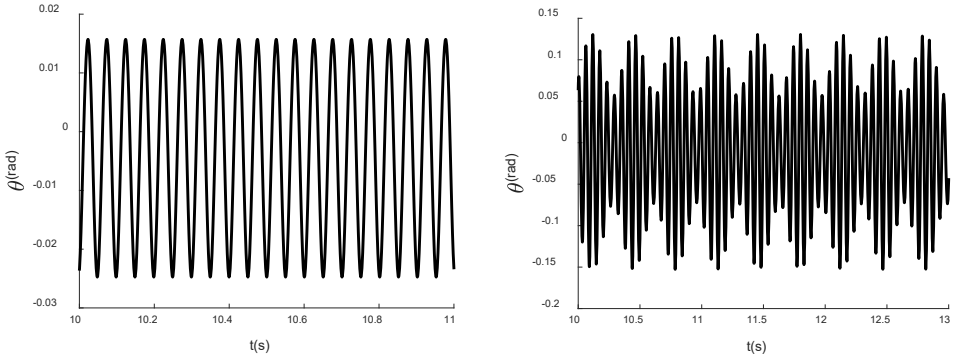

（a）$\tau = 0\text{s}, \sigma = 0.25$ （b）$\tau = 0.015\text{s}, \sigma = 0.25$

Fig. 9 Numerical solution of two different working conditions

Comparing the steady state amplitude in Fig.3 and Fig9, we can find that the numerical solution and analytical solution are basically consistent. With the increase of time delay, the primary resonance amplitude and unstable region also increases. Thus, the time delay of actuator should be controlled to increase the stability of the system while designing wedge brake.

5. CONCLUSION

To analyze the influence of different system parameter and control parameter on braking process of wedge brake, we simplified the friction model based on the Coulomb friction model and smooth function. Then a dynamic model with time-delayed feedback is built for the wedge braking system based on the existing dynamic model. The multiscale method is adopt to obtain the analytical solution of the primary resonance response. The analysis based on the analytical solution show that

1) The cubic term in the governing equation which contains time delay will change the soft or hard characteristics of the response curve. The steady-state amplitude and stability boundary will change periodically at any time. Both the steady state amplitude and the stability boundary have periodic changes vary with time delay. A large time delay in one period will cause the saddle-node bifurcation and unstable solution branch, and finally result in frequency hopping and hysteresis phenomenon.

2) The increase of wedge angle and system stiffness will increase the primary resonance amplitude and expand the unstable region. It can be seen from the results that the parameters such as time delay, wedge angle and system stiffness have a strong influence on the amplitude and stability of the wedge braking system. By appropriately selecting these parameters, the amplitude can be reduced and the stability can be increased.

References

[1] Yao Jian. Research on design, modeling and shifting performance optimization control of wedge clutch. [PhD thesis]. Shanghai: Shanghai Jiaotong University, 2014 (in Chinese)

[2] Jo C H, Lee S M, Song H L, et al. Design and control of an upper-wedge-type electronic brake[J]. Proceedings of the Institution of Mechanical Engineers, Part D: Journal of Automobile Engineering. 2010, 224(11): 1393-1405.

[3] Emam M, Emam A S, El-Demerdash S M, et al. Performance of automotive self reinforcement brake

system[J]. Journal of Mechanical Engineering. 2012, 1(1): 4-10.
[4] Gombert B, Guttenberg P. The electronic wedge brake[J]. ATZ worldwide. 2006, 108(11): 2-5.
[5] Kang J. Automotive brake squeal analysis with rotating finite elements of asymmetric disc in time[J]. Journal of Sound and Vibration. 2017, 393: 388-400.
[6] Stender M, Tiedemann M, Hoffmann N, et al. Impact of an irregular friction formulation on dynamics of a minimal model for brake squeal[J]. Mechanical Systems and Signal Processing. 2018, 107: 439-451.
[7] Chen L, Xi G. Stability and response of a self-amplified braking system under velocity-dependent actuation force[J]. Nonlinear Dynamics. 2014, 78(4): 2459-2477.
[8] Han K, Kim M, Huh K. Modeling and control of an electronic wedge brake[J]. Proceedings of the Institution of Mechanical Engineers, Part C: Journal of Mechanical Engineering Science. 2012, 226(10): 2440-2455.
[9] Mahmoud K, Mourad M. Parameters affecting wedge disc brake performance[J]. International Journal of Vehicle Performance. 2014, 1(3-4): 254-263.
[10] Wang J, Zhang Y, Yang N, et al. Parameters design and braking efficiency analysis of a hydraulic self-energizing wedge disc brake[J]. International Journal of Precision Engineering and Manufacturing. 2017, 18(10): 1409-1418.
[11] Ahmad F, Hudha K, Mazlan S A, et al. Simulation and experimental investigation of vehicle braking system employing a fixed caliper based electronic wedge brake[J]. Simulation. 2018, 94(4): 327-340.
[12] Yu W, Cao J. Hopf bifurcation and stability of periodic solutions for van der Pol equation with time delay[J]. Nonlinear Analysis: Theory, Methods & Applications. 2005, 62(1): 141-165.
[13] Xu Jian, Lu Qiwei. Periodic solution bifurcation and chaos of a non-autonomous time delay feedback control system. Chinese Journal of Mechanics, 2003, 35(4): 443-451 (in Chinese)
[14] Yaman M. Direct and parametric excitation of a nonlinear cantilever beam of varying orientation with time-delay state feedback[J]. Journal of Sound and Vibration. 2009, 324(3-5): 892-902.
[15] Chatterjee S. Time-delayed feedback control of friction-induced instability[J]. International Journal of Non-Linear Mechanics. 2007, 42(9): 1127-1143.
[16] Zhao Yanying. Effect of Time Delay Feedback Control on Vibration Reduction of Vibration System. [PhD Thesis]. Shanghai: Tongji University, 2007 (in Chinese).
[17] Sun X, Xu J. Vibration control of nonlinear Absorber – Isolator-Combined structure with time-delayed coupling[J]. International Journal of Non-Linear Mechanics. 2016, 83: 48-58.
[18] Saha A, Wahi P. An analytical study of time-delayed control of friction-induced vibrations in a system with a dynamic friction model[J]. International Journal of Non-Linear Mechanics. 2014, 63(1-4): 60-70.
[19] Hwang Y, Choi S B. Robust control of electronic wedge brake with adaptive pad friction estimation[J]. International Journal of Vehicle Design. 2013, 62(2): 165-187.
[20] Roberts R, Schautt M, Hartmann H, et al. Modelling and validation of the mechatronic wedge brake[R]. SAE Technical Paper, 2003.
[21] Mahmoud K R, Mourad M, Mahfouz A B. Dynamic behaviors of a wedge disc brake[J]. Applied Acoustics. 2017, 128: 32-39.
[22] Balogh L, Li T S, Meth H N, et al. Modelling and simulating of self-energizing brake system[J]. Vehicle System Dynamics. 2006, 44(sup1): 368-377.
[23] Awrejcewicz J, Grzelczyk D, Pyryev Y. On a Novel Dry Friction Modeling: Differential Equations Computation and Lyapunov Exponent Estimation[C]. 2009.
[24] Duan C, Singh R. Stick-slip behavior in torque converter clutch[J]. Sae Transactions.